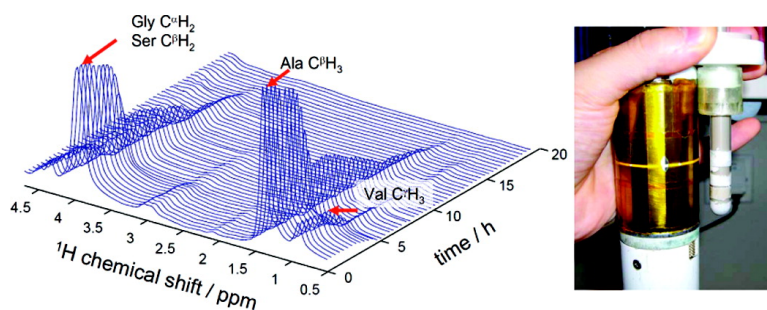


## Investigation of Structural Transition of Regenerated Silk Fibroin Aqueous Solution by Rheo-NMR Spectroscopy

Kosuke Ohgo, Frank Bagusat, Tetsuo Asakura, and Ulrich Scheler

*J. Am. Chem. Soc.*, **2008**, 130 (12), 4182-4186 • DOI: 10.1021/ja710011d

Downloaded from <http://pubs.acs.org> on February 8, 2009



### More About This Article

Additional resources and features associated with this article are available within the HTML version:

- Supporting Information
- Links to the 1 articles that cite this article, as of the time of this article download
- Access to high resolution figures
- Links to articles and content related to this article
- Copyright permission to reproduce figures and/or text from this article

[View the Full Text HTML](#)

## Investigation of Structural Transition of Regenerated Silk Fibroin Aqueous Solution by Rheo-NMR Spectroscopy

Kosuke Ohgo,<sup>†,‡</sup> Frank Bagusat,<sup>‡</sup> Tetsuo Asakura,<sup>\*,†</sup> and Ulrich Scheler<sup>\*,‡</sup>

Department of Biotechnology, Tokyo University of Agriculture and Technology, Koganei, Tokyo 184-8588, Japan, and Leibniz Institute of Polymer Research Dresden, Hohe Strasse 6, D-01069 Dresden, Germany

Received November 5, 2007; E-mail: asakura@cc.tuat.ac.jp; scheler@ipfdd.de

**Abstract:** In this study we applied Rheo-NMR to investigate the structural change of *Bombyx mori* silk fibroin in aqueous solution under shear. Monitoring the time dependence of <sup>1</sup>H solution NMR spectra of silk fibroin subjected to constant shear strain, signal intensities of random coil decreased suddenly during shear while peaks from  $\beta$ -sheet structure did not arise in the solution spectra. After these experiments, an aggregate of silk was found in the Couette flow cell and its secondary structure was determined as  $\beta$ -sheet by <sup>13</sup>C solid-state NMR. In conclusion the moderate shear applied here triggered the change in the secondary structure.

### Introduction

*Bombyx mori* silk fibroin fibers are produced by silkworms at room temperature and from an aqueous solution, but they exhibit exceptional strength, toughness, and resistance to mechanical compression.<sup>1,2</sup> The superiority of the silk fiber is due to not only the nature of the fiber protein but also the processing conditions and higher structure formation through the process as in the processing of synthetic fibers. Silk fibroin also possesses impressive biological properties, giving it considerable potential as a biomaterial for tissue engineering.<sup>3</sup> Consequently, much attention has been focused on the natural mechanism of fiber formation with the aim of understanding how tough fibers are produced naturally and how the process might be mimicked industrially.

The spinning apparatus of the silkworm is an important organ for the fiber formation because spun fibers rely on the extrusion process through the silk press in the spinneret to facilitate molecular orientation and bonding. It has been proposed that fiber formation is mainly induced by shearing and extensional flow in the spinneret.<sup>4</sup> The structural transition of silk molecules occurs from soluble Silk I structure in the spinneret to insoluble Silk II structure in the fiber. The secondary structures for Silk I and Silk II have been proposed as repeated type II  $\beta$ -turn<sup>5,6</sup> and heterogeneous mainly antiparallel  $\beta$ -sheet structure,<sup>7,8</sup> respectively. The fiber formation of silk fibroin depends on the structural change from Silk I to Silk II under external shear forces applying in the spinneret.

To investigate the effect of shear to the aggregation and the fiber formation of silk, rheological studies about silk solutions have been performed.<sup>9–13</sup> Moreover, the structural evolution of aqueous solution of regenerated silk fibroin under shear has been studied in a Couette cell combined with in situ X-ray diffraction methods.<sup>14</sup> Such in situ experiments are a powerful tool for understanding the aggregation process of silk induced by shear.

Rheo-NMR provides the opportunity to study materials or molecules under shear. NMR spectral changes can be followed with moderate time resolution during the application of shear. That can be integral for the entire sample or with spatial resolution. The NMR signal is obtained from inside the material without disturbing the shear experiment. The term Rheo-NMR<sup>15,16</sup> describes NMR experiments of materials under shear, including spectroscopy, imaging, and flow imaging. While in imaging the distribution of individual components in the system under shear and their localized flow are resolved, spectroscopy aims at an understanding of the molecular effects of shear on the molecule. Shear-induced changes in conformation and

<sup>†</sup> Tokyo University of Agriculture and Technology.

<sup>‡</sup> Leibniz Institute of Polymer Research Dresden.

- (1) Asakura, T.; Kaplan, D. L. In *Encyclopedia of Agricultural Science*; Arutzen, C. J., Ed.; Academic Press: New York, 1994; Vol. 4, pp 1–11.
- (2) Shao, Z.; Vollrath, F. *Nature* **2002**, *418*, 741.
- (3) Altman, G. H.; Diaz, F.; Jakuba, C.; Calabro, T.; Horan, R. L.; Chen, J.; Lu, H.; Richmond, J.; Kaplan, D. L. *Biomaterials* **2003**, *24*, 401–416.
- (4) Asakura, T.; Umemura, K.; Nakazawa, Y.; Hirose, H.; Higham, J.; Knight, D. *Biomacromolecules* **2007**, *8*, 175–181.

- (5) Asakura, T.; Ohgo, K.; Komatsu, K.; Kanenari, M.; Okuyama, K. *Macromolecules* **2005**, *38*, 7397–7403.
- (6) Asakura, T.; Ashida, J.; Yamane, T.; Kameda, T.; Nakazawa, Y.; Ohgo, K.; Komatsu, K. *J. Mol. Biol.* **2001**, *306*, 291–305.
- (7) Asakura, T.; Yao, J.; Yamane, T.; Umemura, K.; Ulrich, A. S. *J. Am. Chem. Soc.* **2002**, *124*, 8794–8795.
- (8) Takahashi, Y.; Gehoh, M.; Yuzuriha, K. *Int. J. Biol. Macromol.* **1999**, *24*, 127–138.
- (9) Iizuka, E. *Biorheology* **1966**, *3*, 141–152.
- (10) Yamaura, K.; Okumura, Y.; Ozaki, A.; Matsuzawa, S. *J. Appl. Polym. Sci. Appl. Polym. Symp.* **1985**, *41*, 205–220.
- (11) Holland, C.; Terry, A. E.; Porter, D.; Vollrath, F. *Nat. Mater.* **2006**, *5*, 870–874.
- (12) Terry, A. E.; Knight, D. P.; Porter, D.; Vollrath, F. *Biomacromolecules* **2004**, *5*, 768–772.
- (13) Ochi, A.; Hossain, K. S.; Magoshi, J.; Nemoto, N. *Biomacromolecules* **2002**, *3*, 1187–1196.
- (14) Roessle, M.; Panine, P.; Urban, V. S.; Riekkel, C. *Biopolymers* **2004**, *74*, 316–327.
- (15) Quijada-Garrido, I.; Siebert, H.; Friedrich, C.; Schmidt, C. *Macromolecules* **2000**, *33*, 3844–3854.
- (16) Callaghan, P. *Principles of Nuclear Magnetic Resonance Microscopy*; Clarendon Press: Oxford, 1994; p 512.

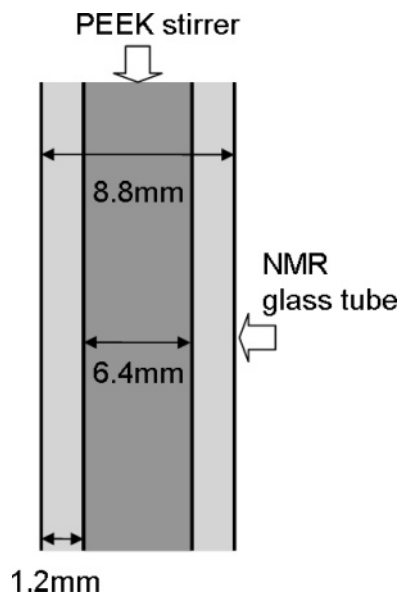


**Figure 1.** Geometry of the rheo cell used for the experiments.

packing would show up in the chemical shift, while alignment and changes in the molecular mobility are revealed by changes in dipolar coupling or relaxation respectively. In this study we applied Rheo-NMR for the investigation of the structural transition of aqueous solutions of regenerated silk fibroin. Time dependence of a series of  $^1\text{H}$  NMR spectra observed under shear provided the information on the structural transition and its kinetics. We also applied the magnetic resonance imaging technique to observe the aggregation process macroscopically.

### Materials and Methods

**Materials.** In order to remove sericin protein from the surface of silk fibers, cocoons of *B. mori* silkworms were degummed three times with 0.25% (w/w) Marseilles soap and with 0.25% (w/w)  $\text{Na}_2\text{CO}_3$  solution at 100 °C for 20 min. Then the silk was washed with distilled water. The silk fibroin fibers were then dissolved in 9.0 M LiBr solution at 40 °C. This solution was dialyzed in distilled water for 4 days at 4 °C. The water was exchanged every 12 h. The final concentration of aqueous silk solution was 5.0 wt %, which was determined by weighing the remaining solid after drying. This aqueous solution was used for an imaging experiment. By lyophilizing the aqueous solution, partially water-soluble silk sponge was generated. The silk sponge was dissolved in  $\text{D}_2\text{O}$  (99%, Sigma-Aldrich), and the remaining insoluble silk was removed by centrifugation (8000 rpm, 10 min). The resulting  $\text{D}_2\text{O}$  solution had a concentration of 2.8 wt % silk. Finally, the pH or pD of the  $\text{H}_2\text{O}$  or  $\text{D}_2\text{O}$  solutions, respectively, were adjusted to a pH  $\approx$  10 by using a pH indicator paper (Merck KgaA, Germany) with an accuracy of about 0.5 units. This pH was chosen to prevent the rapid aggregation of silk fibroin produced by shear under acidic conditions.

**Rheo-NMR Measurements.** Rheo-NMR measurements have been performed on a Bruker Avance 300 NMR spectrometer at a Larmor frequency of 300 MHz for protons, equipped with a microimaging accessory permitting a maximum gradient strength of 1 T/m along three axes. An in-house made rheo cell consisted of a PEEK rotor and NMR glass tube (Figure 1). The rheo cell was placed in a birdcage resonator. The head part of the rotor

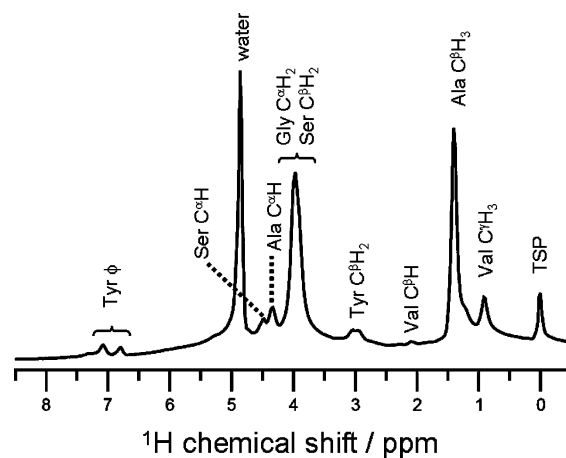


**Figure 2.**  $^1\text{H}$  NMR spectrum of a 2.8 wt % silk fibroin/ $\text{D}_2\text{O}$  solution acquired with the birdcage coil and the rheo cell. The peaks of major amino acid residues in silk fibroin molecules are assigned.

was connected to the driving motor on the top of the NMR magnet. This is the standard Rheo-NMR setup and has been shown to work that the magnet field generated by the motor used is weak. The rotational speed of the inner cylinder was kept constant at 2 Hz. The shear rate in the Couette cell is estimated according to the following equation,

$$\dot{\gamma}(r) = \frac{2\Omega}{r^2 \left( \frac{1}{R_1^2} - \frac{1}{R_2^2} \right)}$$

where  $\Omega$  is angular frequency of the rotor [rad/s],  $R_1$  the outer radius of the rotor, and  $R_2$  inner radius of the glass tube. The parameter  $r$  is the radius from the rotation axis of the rotor ( $R_1 \leq r \leq R_2$ ). From this equation, the shear rate in the cell is calculated as a range of 54–28  $\text{s}^{-1}$  corresponding to  $R_1$  (3.2 mm)  $\leq r \leq R_2$  (4.4 mm). This rotation speed was also used for imaging the distribution of the fibroin along the rotational axis of the cell. A recycle delay of 50 ms for the data acquisition was used. Trimethylsilyl-3-propionic acid sodium salt- $d_4$  (TSP) was used as an internal chemical shift reference and was set to 0 ppm. All measurements were carried out at a temperature of 295 K.

**$^{13}\text{C}$  CP/MAS NMR.** The  $^{13}\text{C}$  CP/MAS NMR measurements were conducted on a Bruker Avance 500 spectrometer operating at 125 MHz for  $^{13}\text{C}$ . A 4 mm rotor at a spinning speed of 5 kHz was used. CP was employed for sensitivity enhancement with high-power  $^1\text{H}$  decoupling during the signal acquisition interval. A  $^1\text{H}$  90° pulse duration of 5  $\mu\text{s}$  was used with 3 ms contact time and 4 s repetition time.  $^{13}\text{C}$  chemical shifts were calibrated indirectly through the adamantane methine peak observed at 28.8 ppm relative to tetramethylsilane at 0 ppm.

### Results and Discussion

**$^1\text{H}$  NMR Spectrum of Silk Fibroin without Shear.** For the assignment of  $^1\text{H}$  peaks in silk fibroin, we measured the  $^1\text{H}$  NMR spectrum of a silk fibroin aqueous solution in the rheo cell without shear. Figure 2 shows the  $^1\text{H}$  NMR spectrum of a 2.8 wt % silk fibroin solution in  $\text{D}_2\text{O}$  with assignment of the peaks, though the resolution in the rheo-imaging probe is inferior

to a high-resolution probe. The amino acid composition of the heavy chain molecule of silk fibroin is 46, 30, 12, 5, and 2 mol % for Ala, Gly, Ser, Tyr, and Val residues, respectively,<sup>17</sup> and the intensity of each  $^1\text{H}$  peak reflects this composition. The  $\text{H}_2\text{O}$  signal was observed from small quantities of  $\text{H}_2\text{O}$  remaining in the silk sponge after lyophilization. In our early works,<sup>18,19</sup> the molecular structure of regenerated silk aqueous solution was determined as random coil structure by  $^{13}\text{C}$  solution NMR. The  $^1\text{H}$  chemical shifts of  $\text{C}^\alpha\text{H}$  in the spectrum are 3.97, 4.33, and 4.48 ppm for Gly, Ala, and Ser residues, respectively, and those of  $\text{C}^\beta\text{H}$  are 1.40, 2.13, and (2.95, 3.03) ppm for Ala, Val, and Tyr residues, respectively. These values closely approximate to random coil  $^1\text{H}$  chemical shifts determined by Bundi and Wuthrich:<sup>20</sup> 3.97, 4.35, 4.50, 1.39, 2.13, and (2.92, 3.13) ppm, respectively. Thus the initial state of the silk molecules in  $\text{D}_2\text{O}$  is determined as random coil structure.

The aggregation of silk fibroin is not only influenced by the external shear forces but also by slow aging, which takes place even at room temperature.<sup>21,22</sup> The self-aggregation of silk fibroin was probed by measuring the  $^1\text{H}$  NMR spectra continuously with a short acquisition time of 3 min for each spectrum. During 36 h, there was no change of intensities and chemical shifts from the first to the last spectrum (data not shown). Thus results obtained from the Rheo-NMR experiments are attributed to the effect of shear.

**Application of Rheo-NMR to Silk Fibroin Solution. Time Dependence of  $^1\text{H}$  NMR Spectra under Shear.** In Figure 3, a typical result obtained from Rheo-NMR measurements for the silk solution is shown.  $^1\text{H}$  signals showed a stepwise time-dependent decay with signal vanishing at 20 h (Figure 3a). After experiment, white flocs were observed in the rheo cell. The production of such flocs by shearing silk solutions has been also reported for regenerated silk solutions<sup>9,14</sup> and silk solutions extracted from the silk glands of silkworms.<sup>11,12</sup> The flocs were analyzed by solid-state NMR, and this was determined as an aggregation of silk molecules with  $\beta$ -sheet structure (vide infra). Furthermore the concentration of the remaining solution in the cell was 0.6 wt %, which has been determined after drying the remaining solution. These observations taken together indicate that the regenerated silk fibroin solution undergoes aggregation, precipitation, and  $\beta$ -sheet formation under shear in the rheometer.

According to the literature by Iizuka,<sup>9</sup> a shear rate at which the fibroin begins to denature to form a fibrous structure is  $14.7 \text{ s}^{-1}$  for 6.3 w/v% regenerated silk fibroin aqueous solution. By using a Couette cell in combination with in situ X-ray methods, it was observed that structural change of the silk fibroin solution occurred at  $300 \text{ s}^{-1}$  with 0.5 w/v % regenerated silk aqueous solution.<sup>14</sup> Here the shear rate of  $28\text{--}54 \text{ s}^{-1}$  derived from a rotation frequency of 2 Hz is comparable to these experiments considering the higher concentration of solutions in our experiment. During compounding and extrusion in

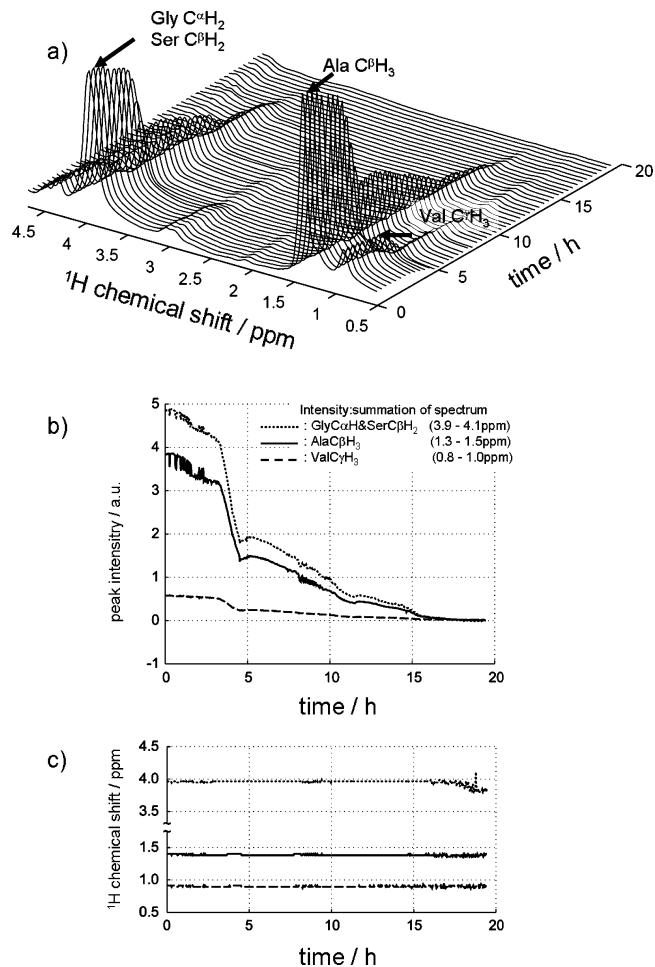


**Figure 3.** (a) Time dependence of a series of  $^1\text{H}$  NMR spectra of a 2.8 wt % silk fibroin/ $\text{D}_2\text{O}$  solution under 2 Hz rotation. Time dependences of (b) intensities and (c) chemical shifts for each peak obtained from a.

synthetic polymer processing, shear rates of  $100 \text{ s}^{-1}$  are typical. In the jet for injection molding or dye extrusion, shear rates of  $1000 \text{ s}^{-1}$  and higher are realized. Even higher shear rates are used for synthetic fiber spinning. By comparison, solidification of silk fibroin occurred at a more moderate shear rate, even in the alkaline conditions we used in which fibroin is likely to be more resistant to shear than in the acidic conditions thought to occur in vivo.

The series of spectra in Figure 3a depicts the time evolution of the  $^1\text{H}$  solution spectra of the silk fibroin under shear. As seen in Figure 3b there are several stepwise decreases of the signal intensity. The intensity of all  $^1\text{H}$  signals attributed to the silk fibroin decrease simultaneously. As shown in Figure 3c, no change of the chemical shift of any signal is observed. Figure 3b and 3c show the time dependences of intensities and chemical shifts for each peak obtained from Figure 3a. The intensities are calculated by the integration of peak area. The chemical shifts are defined by the peak top of each signal. The sudden signal decay is attributed to self-acceleration of the structure change and precipitation triggered by locally enhanced shear rate, because solid silk formed on the rotor locally reduces the width of the gap resulting in a drastically increased shear rate. Half period of random coil is estimated as 4 h from the decay curves. This is much faster than the value of ca. 40 h estimated from the data by Li et al., with addition of preaggregated silks

- (17) Zhou, C.; Confalonieri, F.; Medina, N.; Zivanovic, Y.; Esnault, C.; Yang, T.; Jacquet, M.; Janin, J.; Duguet, M.; Perasso, R.; Li, Z. *Nucleic Acids Res.* **2000**, *28*, 2413–2419.
- (18) Asakura, T.; Watanabe, Y.; Uchida, A.; Minagawa, H. *Macromolecules* **1984**, *17*, 1075–1081.
- (19) Asakura, T. *Makromol. Chem. Rapid Commun.* **1986**, *7*, 755–759.
- (20) Bundi, A.; Wuthrich, K. *Biopolymers* **1979**, *18*, 285–297.
- (21) Matsumoto, A.; Chen, J.; Collette, A. L.; Kim, U. J.; Altman, G. H.; Cebe, P.; Kaplan, D. L. *J. Phys. Chem. B* **2006**, *110*, 21630–21638.
- (22) Li, G. Y.; Zhou, P.; Shao, Z. Z.; Xie, X.; Chen, X.; Wang, H. H.; Chunyu, L. J.; Yu, T. Y. *Eur. J. Biochem.* **2001**, *268*, 6600–6606.

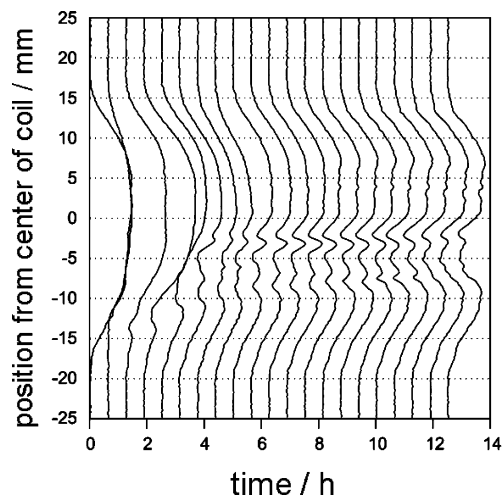


**Figure 4.** Time dependence of the distribution of H<sub>2</sub>O along the length of the rotor obtained from a 5.0 wt % silk fibroin/H<sub>2</sub>O solution.

without shear.<sup>22</sup> The kinetics also suggest that the shear accelerates the aggregation process. Additionally, curves normalized by their initial intensities are almost consistent with each other. Especially, Val residues mainly dominate their positions in the amorphous, nonrepetitive regions in the primary sequence of silk fibroin while the amino acid sequence of the  $\beta$ -sheet forming crystalline region is dominated by the sequence (Gly-Ala-Gly-Ala-Gly-Ser)<sub>n</sub>.<sup>17</sup> Thus, similar time course diminutions imply that there is no site-specific on the aggregation process, i.e., a preceding aggregation in the crystal regions does not exist.

Contrary to the rapid change of intensities, there was almost no change in <sup>1</sup>H chemical shifts of each peak. As shown below, the drastic structural transition from random coil to rigid  $\beta$ -sheet is clearly induced by shear. Then of particular interest is an intermediate state between the two states, random coil and predominantly  $\beta$ -sheet. In the present Rheo-NMR experiments, only a signal from dissolved protein is obtained, the solid fraction does not contribute. However, a change in the secondary shift would be observable in, for example, Gly C <sup>$\alpha$</sup> H<sub>2</sub> (0.5 ppm).<sup>23</sup> The fact that no change in Gly C <sup>$\alpha$</sup> H<sub>2</sub> has been observed indicates that no  $\beta$ -sheet intermediate exists in the solution. It is concluded there is an instantaneous transition from random coil to  $\beta$ -sheet and this secondary structure change results in sudden precipitation.

As the aqueous solution obtained by the dialysis contains only 5.0% fibroin, only the solvent needs to be considered for an imaging experiment. Figure 4 shows how the distribution of H<sub>2</sub>O changes along the length of the rotor with time. The initial image shows a uniform distribution along the length of the rotor. The reduced local intensities developing during the course of the experiment are an indication that the water is displaced by solid silk formed on the rotor as seen after the experiment. The solid phase has been the subject of <sup>13</sup>C CP/MAS NMR investigation.

**Solid-State NMR Analysis of Aggregated Silk.** The molecules of *B. mori* silk fibroin take several kinds of structures in the solid state, namely Silk I, Silk II, and random coil structure. Silk I is obtained by gently evaporating of an aqueous solution

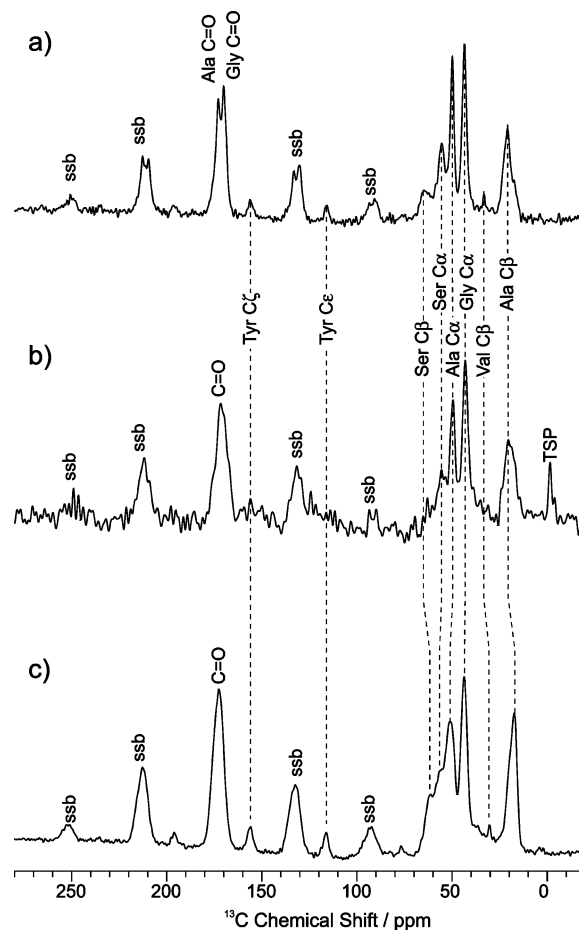


**Figure 5.** <sup>13</sup>C CP/MAS solid-state NMR spectra of (a) silk fiber after degumming, (b) aggregates appeared in the rheo cell after Rheo-NMR experiment, and (c) lyophilized silk sponge. Spinning sidebands are indicated by 'ssb'.

and is defined as repeated type II  $\beta$ -turn structure. Silk II is the molecular structure in the fiber, and it is proposed as a heterogeneous mainly antiparallel  $\beta$ -sheet. Silk fibroin with random coil structure is obtained by, for example, lyophilization of the aqueous solution. In the solid state <sup>13</sup>C NMR spectra, those structures give characteristic chemical shifts in both backbone and side chain carbon peaks. Thus, it is easy to distinguish the secondary structure of silk aggregate after Rheo-NMR measurements by solid-state <sup>13</sup>C NMR. In Figure 5, a <sup>13</sup>C CP/MAS NMR spectrum of silk aggregate is shown with that of the fiber and the lyophilized sponge. Peak positions of the aggregate in the aliphatic region are almost consistent with that of the silk fiber. It is well-known that the chemical shift of Ala C <sup>$\beta$</sup>  peak shows a strong dependence of the secondary structure.<sup>24,25</sup> The Ala C <sup>$\beta$</sup>  peak in the aggregated material has a similar position compared with the silk fiber. Thus, the evidence of  $\beta$ -sheet structure is demonstrated.

The <sup>13</sup>C chemical shift of carbonyl carbons reflects the state of hydrogen bond in the secondary structure.<sup>26–28</sup> For example,

- (24) Iwadata, M.; Asakura, T.; Williamson, M. P. *J. Biomol. NMR* **1999**, *13*, 199–211.  
 (25) Asakura, T.; Iwadata, M.; Demura, M.; Williamson, M. P. *Int. J. Biol. Macromol.* **1999**, *24*, 167–171.  
 (26) Ando, S.; Ando, I.; Shoji, A.; Ozaki, T. *J. Am. Chem. Soc.* **1988**, *110*, 3380–3386.  
 (27) Asakawa, N.; Kuroki, S.; Kurosu, H.; Ando, I.; Shoji, A.; Ozaki, T. *J. Am. Chem. Soc.* **1992**, *114*, 3261–3265.  
 (28) Kameda, T.; Takeda, N.; Kuroki, S.; Ando, S.; Ando, I.; Shoji, A.; Ozaki, T. *J. Mol. Struct.* **1996**, *384*, 17–23.

(23) Wishart, D. S.; Sykes, B. D.; Richards, F. M. *J. Mol. Biol.* **1991**, *222*, 311–333.

there are chemical shift differences of 7 and 3 ppm between Gly and Ala carbonyl peaks in Silk I and Silk II structures, respectively.<sup>6,7</sup> This carbonyl chemical shifts reflect a different state of hydrogen bond in two structures, i.e., both intra and intermolecular hydrogen bond in Silk I (repeated type II  $\beta$ -turn) and fully intermolecular hydrogen bond in Silk II (antiparallel  $\beta$ -sheet). As shown in Figure 4, the widths of Gly and Ala carbonyl carbons in the silk fiber are very sharp and two peaks are completely separated. This suggests the presence of a well ordered state of hydrogen bonds. On the other hand, one broad peak is observed in both the aggregate and the lyophilized sponge. This implies that the hydrogen bonds are ordered in the fiber but not in the aggregate. The difference of the state of hydrogen bond between the fiber and the aggregate may be attributed to the state of the solution before aggregation. The concentration of the silk solution is around 30 wt %<sup>13</sup> or higher through the silk glands to the spinneret, and molecules are closely packed to each other. Moreover, it is suggested that the silk solution is in a liquid crystal phase in the spinneret.<sup>4,29</sup> Under these conditions, the silk molecules are aligned before aggregation, and ordered hydrogen bonds are formed. On the other hand,

(29) Willcox, P. J.; Gido, S. P.; Muller, W.; Kaplan, D. L. *Macromolecules* **1996**, *29*, 5106–5110.

in our experimental system the concentration is lower than in the native state, and the conformation is mainly a random coil structure. The transition from the random coil structure may induce a more disordered  $\beta$ -sheet structure in the aggregate.

## Conclusions

Rheo-NMR was applied to investigate the shear-induced structural transition of an aqueous *B. mori* silk fibroin solution. In this study, the transition from random coil to  $\beta$ -sheet was successfully observed. The concentration of silk solution decreases, and the development of the aggregates was observed synchronously by using <sup>1</sup>H signal projections. There are a lot of NMR techniques to detect molecular structure, organization, and dynamics, which can be combined with Rheo-NMR and would enable further insights in the structural transition of silk fibroin.

**Acknowledgment.** T.A. acknowledges support from Grants-in-Aid for Scientific Research (S) (No. 18105007), Japan. U.S. acknowledges the BMBF for initial financial support under grant 03N8624.

JA710011D